J Appl Electrochem (2014) 44:1117–1125
DOI 10.1007/s10800-014-0733-8

RESEARCH ARTICLE

Influence of temperature on the properties of Mn coatings electrodeposited from the electrolyte containing Te(VI) additive

E. Griškonis · A. Šulčius · N. Žmuidzinavičienė

Received: 19 May 2014 / Accepted: 18 August 2014 / Published online: 27 August 2014

Abstract The influence of the bath temperature on composition, current efficiency, structure, morphology, internal stresses and microhardness of Mn coatings obtained from manganese-ammonium sulphate electrolyte with 2.20 mM of Te(VI) additive at the current density of 15 A dm^{-2} was investigated. It has been found that with rising of the bath temperature from 20 to 80 °C the current efficiency increases from 37 to 71 %, the total concentration tellurium in the deposits increases from 0.9 to 1.6 wt% and the average size of crystallites of the coatings declines approx. from 24 to 15 nm. The structure of Mn coatings changes from the mixture of α-Mn and β-Mn phases at the lower temperatures to α-Mn phase at higher temperatures. Large tensile stresses (from 76 to 106 MPa) were determined for the Mn coatings with the thickness of 1.5–2.0 μm obtained at the initial stage of the deposition process.

Keywords Electrodeposition of manganese · Manganese(II)-ammonium sulphate bath · Te(VI) additive · Morphology · Mechanical properties

1 Introduction

Manganese is the most electronegative metal ($E^{\circ}_{Mn^{2+}/Mn} = -1.18$ V vs. SHE) that can be electrodeposited from aqueous solution. The electrowining is the main process for obtaining high purity metallic manganese, which is mainly used as alloying component for the production of various steals and non-ferrous alloys [1, 2]. In galvanoplastic, Mn electrodeposits are potentially useful as sacrificial coatings for protecting ferrous substrates against corrosion [3]. In most cases, electrodeposition of manganese can be performed from acidic chloride [3–13]. Ammonium salts are indispensable components in these baths for obtaining manganese electrodeposits of the sufficient quality. Rather fast corrosion of manganese coatings and high rate of hydrogen evolution on these coatings in above mentioned electrolytes are the main disadvantageous processes during manganese electrodeposition [4, 14]. This leads to the significant low current efficiency of manganese electrodeposits. Only using some compounds of chalcogens, i.e. sulphur [7, 14], selenium [15–20] and tellurium [21–23] as additives in manganese electrolyte allows to electrodeposit Mn coatings of good quality and with the moderate or quite high current efficiency. There are only few reports on the investigations of the influence of tellurium compounds (mostly Te(IV)) on the manganese electrodeposition from the bath containing manganese(II) and ammonium sulphates (MASB).

The literature data on microhardness and internal stress of some electrodeposited metals are not numerous [24]. Microhardness is sensitive to purity of the solutions and depends on the thickness and purity of the deposits as well as on other factors. It should be noted that the Mn, electrodeposited from sulphate electrolyte without additive, characterized by tensile stresses [25]. It is known, that the quality of the metals and alloys coatings and their adhesion with substrate leads the internal stresses [26]. Compression stresses of coatings can cause the coating delamination from the substrate [27], and the tensile stresses can cause cracks of coatings [28].

E. Griškonis (✉) · A. Šulčius · N. Žmuidzinavičienė
Department of Physical and Inorganic Chemistry, Kaunas University of Technology, Radvilenu pl. 19, 50254 Kaunas, Lithuania
e-mail: egidijus.griskonis@ktu.lt

The aim of the present work was investigation of the influence of the temperature on the electrodeposition process of Mn coatings from MASB containing Te(VI) additive and estimation of their properties.

2 Experimental

The aqueous electrolyte of the following composition was used as MASB: 0.95 M ammonium sulphate ($(NH_4)_2SO_4$, Reakhim, 99.0 %) and 0.62 M manganese(II) sulphate ($MnSO_4{\cdot}5H_2O$, Reakhim, 99.0 %). The twice-distilled water was used for the preparation of MASB. Sodium tellurate ($Na_2TeO_4{\cdot}2H_2O$, Aldrich, 99.5 %) was used as Te(VI) additive in MASB. Since we have reported previously [23] that the best quality, semi-glossy Mn coatings were obtained from MASB with Te(VI) additive of 2.20 mM concentration at room the temperature and at cathodic current density (j_c) of 15 A dm^{-2}, all the electrodeposition experiments at the elevated temperatures were performed at the above mentioned additive concentration and current density. Duration of electrodeposition at this constant current density was 8 min and this corresponded to charge of 7,200 coulombs dm^{-2}.

It should be emphasized that the stable MASB with Te(VI) additive could be obtained only in the strongly acidic media. The preparation of such acidic electrolyte (pH $\sim$2.3) was described in detail in our previous paper [23]. The adjustment of pH of MASB was performed with aqueous solutions of ammonia (35 wt%) and sulphuric acid (35 wt%) using laboratory pH-meter WTW330 with the combined electrode SenTix®41 (Germany) at 20±1 °C. The electrolyte was not stirred during all the processes of electrodeposition.

Mild carbon steel (St-3 (GOST 380-94), equivalent to steel ASTM 570 grade 36, contain 0.22 % C, 0.5 % Mn, 0.1 % Si, <0.04 % P, <0.05 % S) plates (20 × 20 mm), were used as cathodes for the electrodeposition of Mn coatings. The surfaces of the electrodes were polished with felt wheel by using Cr_2O_3 polishing paste, degreased by Vienna lime and etched for 10–15 s in the solution of sulphuric acid (2 %) immediately before electrodeposition process. Pb-1 %Ag alloy plates coated with a MnO_2 film were used as insoluble anodes. Such anodes are widely used for the electrodeposition of Mn and its alloys (Ni–Mn, Zn–Mn) [29, 30] and Zn coatings in industry [31, 32]. They were produced by alloying pure Pb with an appropriate amount of pure Ag powder and subsequently by anodically pretreatment in MASB with a small amount of NH_4Br as an additive. Diaphragms of polyvinyl chloride fabric were used for the separation of cathodic and anodic compartments of the electrodeposition cell. The required increase in temperature (±1°C) of electrolyte in the cell was maintained with a coil in which hot water of the appropriate temperature circulated from the thermostat.

The estimation of the concentrations of Te and Mn in the coatings was carried out by atomic absorption spectroscopy (AAS) using Perkin Elmer model 503 spectrophotometer. For the measurements of Mn and Te concentrations in the coatings, they were dissolved in the minimal volume of dilute HNO_3 (ca. 15 wt%) solution and made up to the mark of the measuring flask with dilute HCl solution (1 wt%). The standard solutions of Mn and Te were prepared according to the procedure described in the special literature of the supplier of AAS technique [33].

The structure of electrodeposits was investigated by X-ray diffraction analysis (XRD) using Bruker D8 Advance diffractometer. In accordance with the X-ray data the diffraction patterns of Mn coatings were identified using Bruker AXS software (program EVA), and PDF-2 database. The calculation of average crystallite size was performed in a conventional way according to the Scherrer formula after the measurements of the full widths at the half maxima of the peaks in the X-ray diffractograms using computer program X-fit. The reliability of the method reached 98 %.

The morphology of electrodeposits was investigated by atomic force microscopy (AFM) with microscope NT 206 (Belarus) by scanning a surface area of 12 × 12 μm of a sample in air using the contact mode. The investigation of morphology of the surface of the electrodeposits was performed using FEI Qanta 200 FEG scanning electron microscope (SEM) with Bruker XFlash® 4030 detector for high resolution energy dispersive X-ray (EDX) spectroscopy also.

Microhardness by Vickers and internal stresses of Mn coatings were measured by the methods which were described in detail in our previous paper [23].

3 Results and discussion

3.1 Composition and current efficiency

The compositional analysis performed by AAS has shown that with the increase of the temperature of MASB with Te(VI) additive from 20 to 80 °C, the total concentration of Mn in the obtained coatings remains almost constant and varies slightly from 98 to 99 wt%. Meanwhile, the concentration of incorporated Te in the obtained coatings increased from 0.9 to 1.6 wt% (Fig. 1). Incorporation mechanism of Te into Mn coatings and the influence of Te

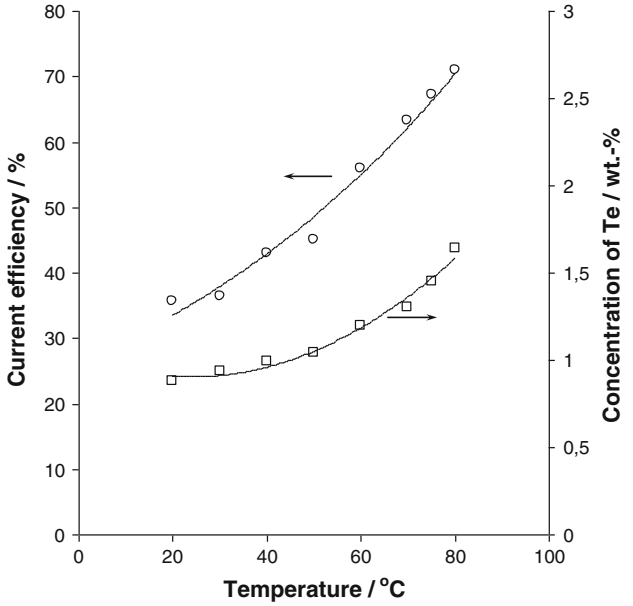

Fig. 1 Influence of temperature on Te concentrations (wt%) in Mn coatings and current efficiency of coatings obtained from MASB with 2.20 mM Te(VI) additive at $j_c = 15$ A dm^{-2}

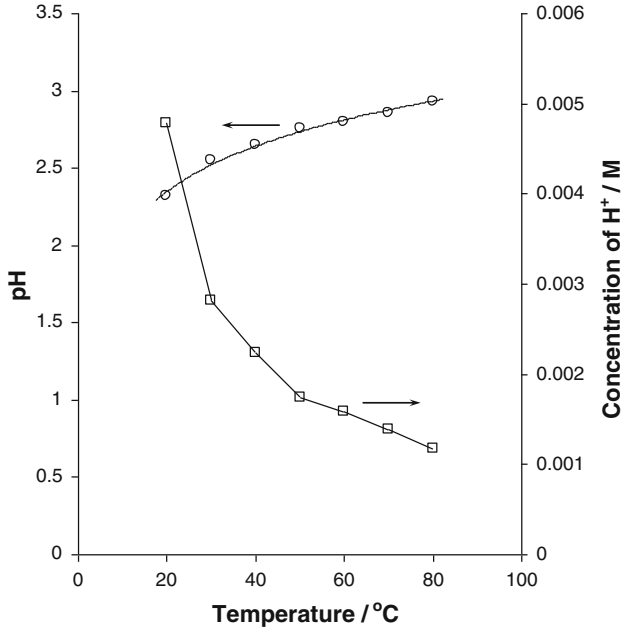

Fig. 2 Influence of temperature on pH and molar concentration of hydrogen ions [H^+] in non-electrolysed MASB containing 2.20 mM of Te(VI) additive. Initial pH value of MASB prepared at room temperature (20 °C) was ~2.3

or its compounds on electrodeposition process of Mn were discussed thoroughly enough in several papers [21, 22].

It was observed that the current efficiency of the coatings electrodeposited at the $j_c = 15$ A dm^{-2} showed weak exponential dependence on the temperature and its values increased almost twice (from 37 to 71 %) when the temperature of MASB increased from 20 to 80 °C (Fig. 1). The average thickness of Mn coatings at the same time increased from 9.8 to 19.5 μm. Increasing of current efficiency can be partially explained by the increase of pH value of MASB with the rising of the temperature. The concentration of hydrogen ions in MASB decreased exponentially by ca. four times when the temperature of MASB increased from 20 to 80 °C (Fig. 2).

Increasing of pH (and respectively decreasing of concentration of H^+ ions) with the rising of temperature of MASB are concerned with phenomenon of hydrolysis and peculiarity of manganese and sulphate ions interaction in water solution. On the one hand, hydrated manganese ions participate in the hydrolysis reaction (1) and that lead to the weakly acidic medium of solution:

$$\left[Mn(H_2O)_6\right]^{2+}_{(aq)} \rightleftarrows \left[Mn(H_2O)_5(OH)\right]^{+}_{(aq)} + H^{+}_{(aq)} \quad (1)$$

On the other hand, the rising of temperature decrease dielectric constant of the water, and this leads to a stronger electrostatic interaction between the opposite charged ions in solution [34]. Thus, increasing of temperature could promote the association of divalent manganese Mn^{2+} and sulphate SO_4^{2-} ions with forming so-called "solvent-shared ion pair" and "contact ion pairs" in water solutions (2) [35]:

$$\underset{\text{Separated fully solvated ions}}{\left[Mn(H_2O)_6\right]^{2+}_{(aq)} + SO^{2-}_{4(aq)}} \rightleftarrows \underset{\text{Solvent - shared ion pair}}{\left[Mn(H_2O)_6\right]SO_{4(aq)}} \rightleftarrows \underset{\text{Contact ion pair}}{\left[Mn(H_2O)_5(SO_4)_{(aq)}\right]} + H_2O_{(l)} \quad (2)$$

Increasing of ionic association constant with rising of temperature has been clearly established for similar (2+):(2−) type electrolyte $CuSO_4$ in aqueous solution [36].

Most probably in the case of MASB, the rising of pH with increasing of temperature could be explained by the releasing of OH^- ions, when penthaaqua manganese(II) hydroxide ions $\left[Mn(H_2O)_5(OH)\right]^{+}_{(aq)}$ participate in contact ion pairs formation (3). Released hydroxide OH^- ions neutralize hydrogen H^+ ions and thus increasing pH of MASB.

$$\underset{\text{Separated fully solvated ions}}{\left[Mn(H_2O)_5(OH)\right]^{+}_{(aq)} + SO^{2-}_{4(aq)}} \rightleftarrows \underset{\text{contact ion pair}}{\left[Mn(H_2O)_5(SO_4)_{(aq)}\right]} + OH^{-}_{(aq)} \quad (3)$$

Table 1 Influence of temperature on pH of aqueous solutions of MASB and basic MASB components (without Te(VI) additive)

Temperature (°C)	pH		
	0.62 M $MnSO_4$ + 0.95 M $(NH_4)_2SO_4$	0.95 M $(NH_4)_2SO_4$	0.62 M $MnSO_4$
20	3.60	5.90	3.18
30	3.77	5.74	3.35
40	3.91	5.53	3.49
50	4.00	5.32	3.60
60	4.05	5.12	3.69
70	4.09	4.96	3.78
80	4.10	4.83	3.86

Here should be emphasized that the nature of hydration of sulphate anions, presented in reactions (2) and (3), is determined by formation of weak hydrogen bonds (not donor–acceptor coordinating bond as in case of hydrated metal ion). Hydration shell of sulphate anion is composed of small rings of hydrogen bonded water molecules [37].

To clarify the influence of basic MASB components ($MnSO_4$ and $(NH_4)_2SO_4$) on changing of pH with increasing of temperature were made additional measurements of pH values of aqueous solutions of individual salts and their mixture at different temperatures (Table 1).

Furthermore, it is known that during electrodeposition pH value near cathode layer can increase up to one unit (i.e. concentration of $H^{+}_{(aq)}$ ions decreases by ca. ten times) in MASB at the room temperature [38]. Thus, decreasing of concentration of hydrogen ions in MASB leads to the significant drop of partial discharging current of $H^{+}_{(aq)}$ ions and to the decrease of evolution rate of gaseous hydrogen on the Mn electrodeposit. On the other hand, the increased concentration of Te incorporated into Mn coatings, observed at the higher temperatures, could additionally reduce the self-dissolving (corrosion) rate of Mn in acidic MASB [6, 39, 40].

The surface analysis of Mn coatings performed by EDX in the "point mode" (together with SEM analysis) showed that surface concentration of Te differs on the lower and on the upper parts of the morphology (on the pits and on the bumps, respectively). Such a difference was also observed in our previous paper [23]. The biggest differences of Te concentration in upper and lower parts of morphology were observed for coatings obtained from MASB at the lower temperatures (Fig. 3). The difference of Te concentrations decreases with the increase of the temperature of MASB. This observation can apparently be explained by the formation of smoother Mn coatings at the elevated temperatures. This assumption was confirmed by the measurements of the roughness performed with AFM. The difference in Te concentrations determined by the different techniques (AAS and EDX) is related to the morphological artefacts of intrinsically local quantitative EDX analysis, especially for alloys [41].

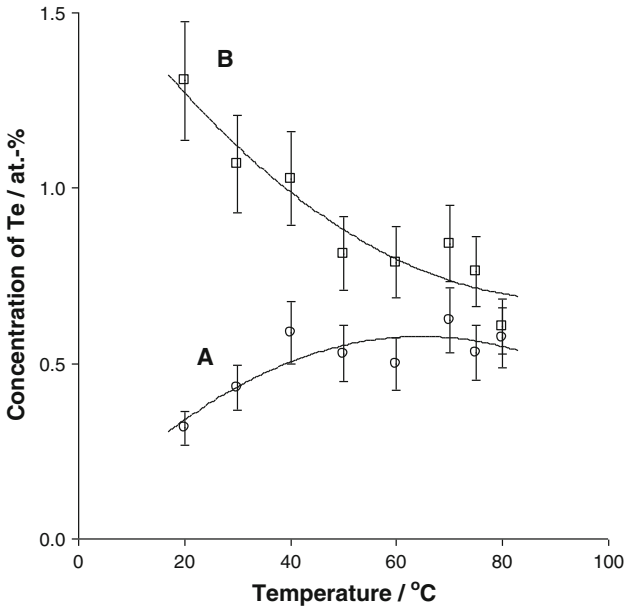

Fig. 3 Influence of temperature on distribution of Te in upper (curve *A*) and lower (curve *B*) parts of morphology of Mn coatings obtained from MASB with 2.20 mM of Te(VI) additive at $j_c = 15$ A dm^{-2}

3.2 X-ray diffraction study and morphology

As it was mentioned above, Te incorporates into Mn coatings and changes their structure and morphology. XRD analysis showed that the coating obtained at $j_c = 15$ - A dm^{-2} at the room temperature (20 °C) consists of the mixture of two phase modifications: hard and brittle α-Mn (body-centered cubic) phase and plastic β-Mn (cubic) phase. The smooth changes in the structure were observed for Mn coatings obtained from MASB with Te(VI) additive

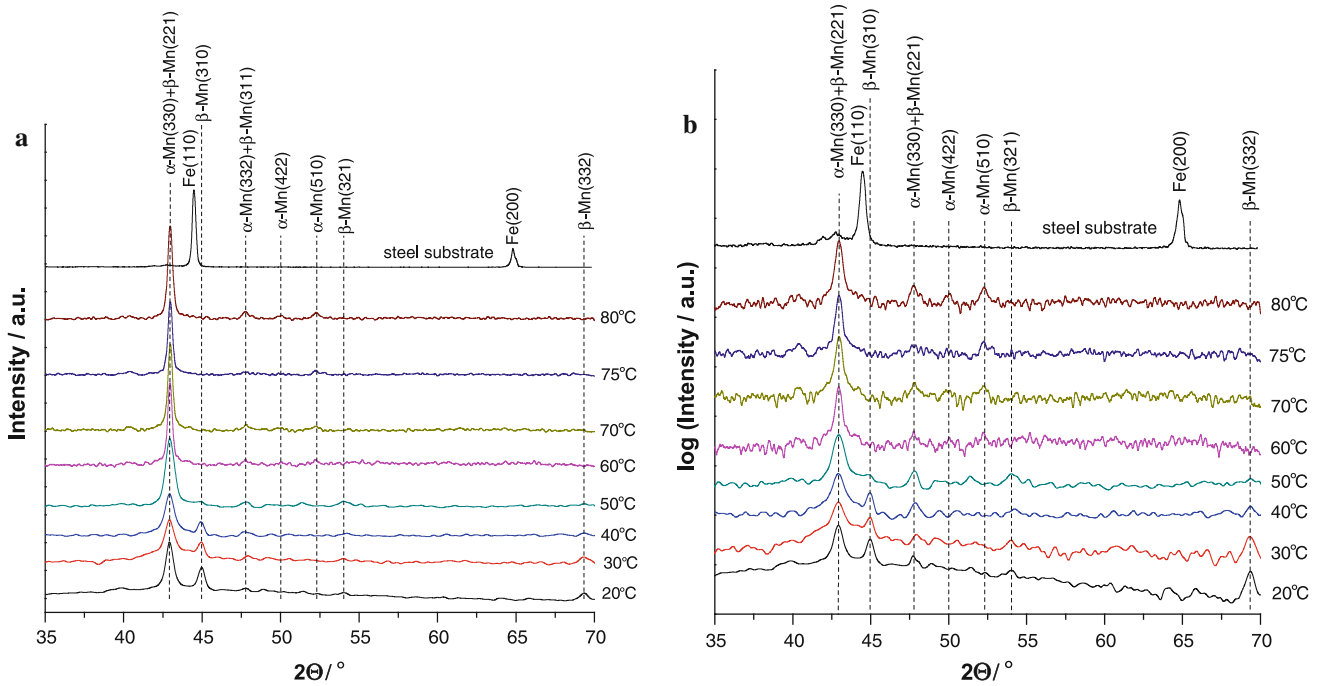

Fig. 4 X-ray diffraction patterns of Mn coatings obtained from MASB with 2.20 mM of Te(VI) additive at $j_c = 15$ A dm^{-2} and different temperatures: **a** linear scale of intensity; **b** logarithmic scale of intensity

at the increased temperatures (30–50 °C). When the temperature of MASB was higher than 40 °C, the structure of Mn coatings changed considerably (Fig. 4): β-Mn phase (characteristic peaks at 2Θ ~45° and ~69°) disappeared and the harder α-Mn phase remained. Such a change was also observed by other authors [42] when electroplating at 60 °C produced deposits composed completely of the α-Mn phase.

The calculation of the average size of the crystallites showed that the coatings obtained from MASB with Te(VI) additive at $j_c = 15$ A dm^{-2} and in full range of the chosen temperatures are nanocrystalline (Fig. 5). The variation of the full width at half maximum of all suitable for calculation peaks of α-Mn and β-Mn phases (individual and mixture) indicated that average size of crystallites decreased with the increase of the temperature of MASB. The average size of crystallites of Mn coatings obtained at 20 °C was found to be ca. 24 nm, whereas the size of crystallites reached only approx. 15 nm at the highest temperature (80 °C). The similar decrease of the surface roughness and average height values of Mn coatings with the increase of MASB temperature was observed by AFM (Fig. 6; Table 2).

Figure 7 illustrates the changes of morphology of Mn coatings, obtained from MASB with the additive of Te(VI) at $j_c = 15$ A dm^{-2} observed at the different temperature. The SEM images showed the uncertain form of fine grains on the surface of Mn deposits obtained at 20–40 °C. When

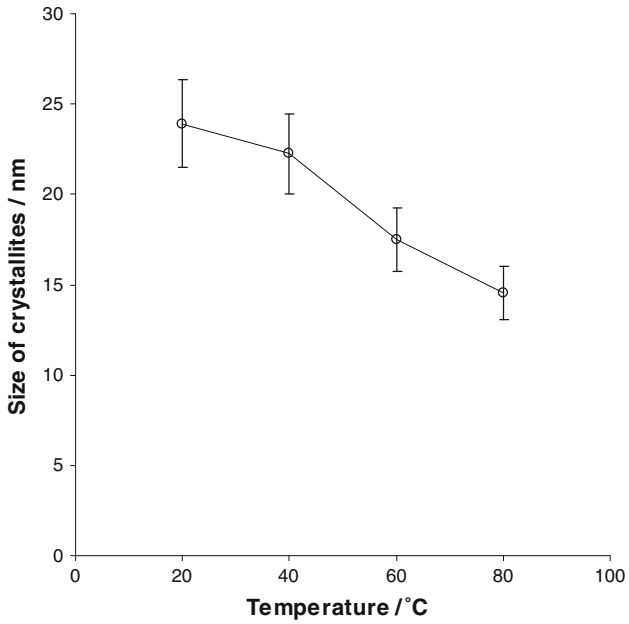

Fig. 5 Influence of temperature on average crystallites size of Mn coatings obtained from MASB with 2.20 mM Te(VI) additive at $j_c = 15$ A dm^{-2}. Calculations were performed by taking into account all suitable for calculation peaks

the temperature of MASB was 50 °C and higher, the cube-shaped grains of various dimensions appeared on the surface of the obtained Mn coatings. This is quite natural,

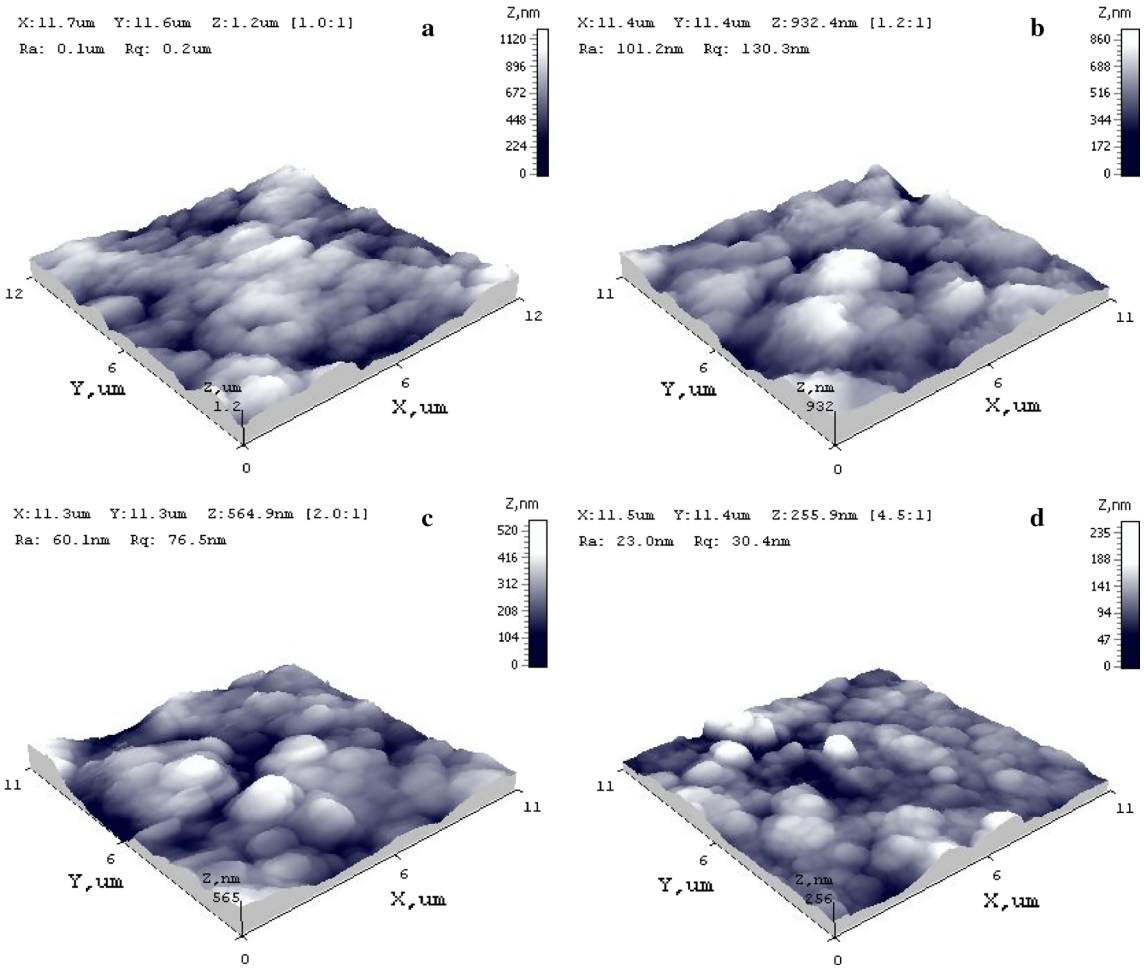

Fig. 6 3D topographic AFM images of Mn coatings obtained from MASB with 2.20 mM of Te(VI) additive at $j_c = 15$ A dm^{-2} and different temperature: **a** 20 °C; **b** 40 °C; **c** 60 °C; **d** 80 °C

Table 2 Roughness, average height and skewness values detected by AFM for Mn coatings, obtained from MASB with 2.20 mM Te(VI) additive at $j_c = 15$ A dm^{-2} and different temperatures

Dimension	Temperature (°C)			
	20	40	60	80
Root mean square roughness R_q (nm)	178.57	130.28	76.48	30.39
Average roughness R_a (nm)	145.10	101.20	60.12	23.05
Average height Z_{mean} (nm)	682.15	562.23	269.33	115.15
Skewness R_{sk}	−0.15	−0.20	0.03	0.48

because cubic structure of lattice is characteristic for manganese (for both α-Mn and β-Mn phases) [43, 44].

3.3 Mechanical properties

The previous study [23] showed that the increasing of the cathodic current densities from 2 to 15 A dm^{-2} lead to exhibition of large tensile stresses in Mn coatings obtained from MASB with Te(VI) additive at the room temperature. In the present study, the tensile stresses were estimated only for Mn coatings obtained in the temperature range from 20 to 60 °C. The experimental data of tensile stresses at temperature 70 °C and higher could not be accessed because of technical limitations (increased evaporation of water from electrolyte leads to adverse event, i.e. water steam condensation on the optical parts of microscope of the measuring equipment and this was hinder the measurement). Figure 8 shows that with increasing of the temperature of the electrolyte, the maximum tensile stress values of the obtained Mn coatings decreased from 106 to 76 MPa (measured at 20 and 60 °C, respectively). In the whole temperature range chosen, as well as at 20 °C, the maximum tensile stress values of the obtained Mn electrodeposits were observed at the initial period of the formation, i.e. when thickness of Mn coatings was 1.5–2.0 μm. The slight

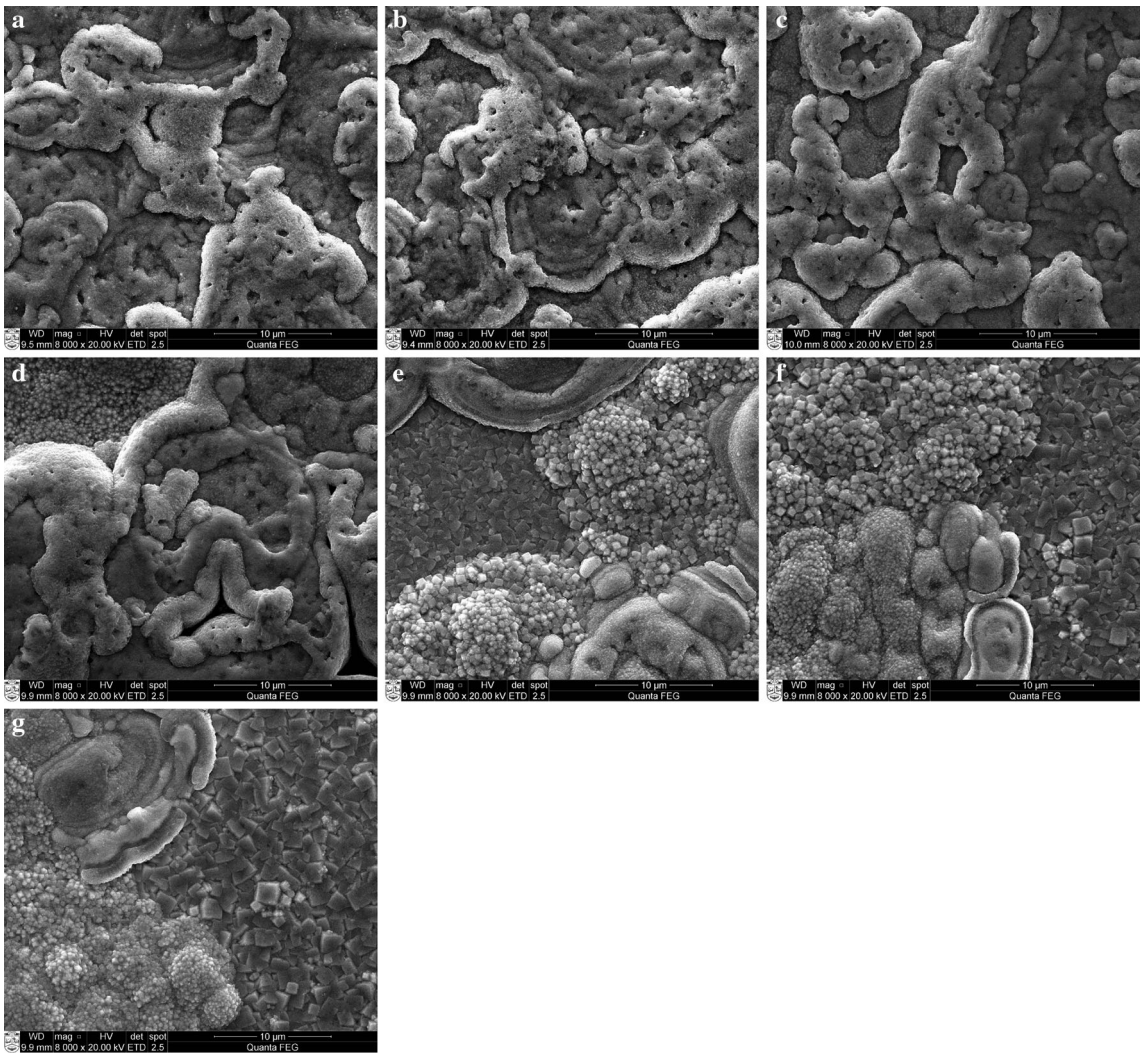

Fig. 7 SEM images of Mn coatings obtained from MASB with 2.20 mM of Te(VI) additive at $j_c = 15$ A dm^{-2} and different temperature: **a** 20 °C; **b** 30 °C; **c** 40 °C; **d** 50 °C; **e** 60 °C; **f** 70 °C; **g** 80 °C. Magnitude ×8,000

relaxation of tensile stresses was observed with the increase of the thickness of electrodeposits.

Microhardness by Vickers of Mn coatings obtained from MASB with Te(VI) additive at the $j_c = 15$ A dm^{-2} was tested in the full range of the temperatures (Fig. 9). Increase of the temperature from 20 to 50 °C of MASB lead to the decrease of microhardness of Mn coatings from 1,820 MPa to 1,452 MPa. It is apparently related with the structural changes of the coatings containing the mixture of α-Mn and β-Mn phases. The values of microhardness of Mn coatings obtained at higher temperatures increased considerably from 1,984 MPa (at 60 °C) to 2,772 and 3,700 MPa (at 70 and 80 °C , respectively). This observation can apparently be explained by the increase of the total concentration of Te in Mn electrodeposits and by predomination of the hardened α-Mn phase in them [45].

4 Conclusions

The increase of the temperature of manganese ammonium sulphate bath containing 2.20 mM of Te(VI) additive from 20 to 80 °C leads to the changes of various characteristics and properties of Mn coatings obtained at current density of 15 A dm^{-2}.

The total concentration of the incorporated Te into the obtained Mn coatings increased from 0.9 to 1.6 wt% with rising of bath temperature. The EDX analysis of surface of electrodeposits performed in "point mode" showed the different surface concentrations of Te on the lower and on the upper parts of the layers. The differences decreased with the increase of the temperature of manganese ammonium sulphate bath. This observation is explained by the surface smoothening of Mn coatings at higher temperatures. The effect of the increased temperature on the

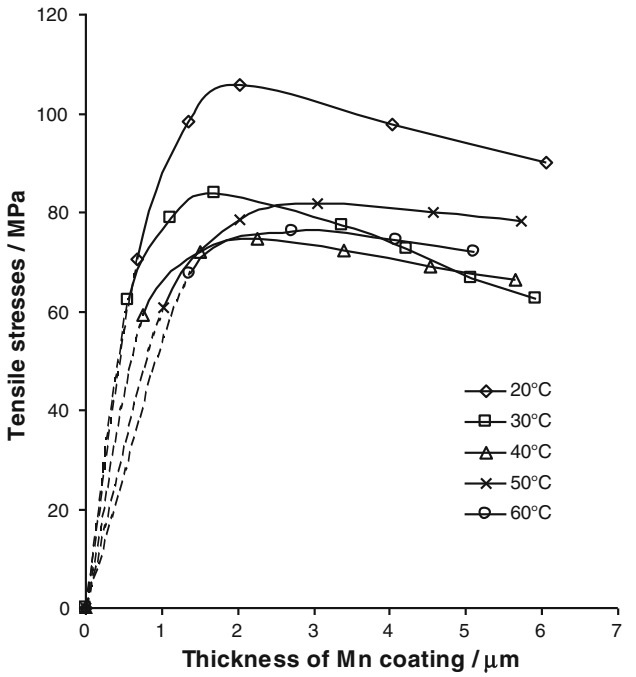

Fig. 8 Dependence of tensile stresses on thickness of Mn coatings obtained from MASB with 2.20 mM of Te(VI) additive at $j_c = 15$ - A dm^{-2} and different temperature

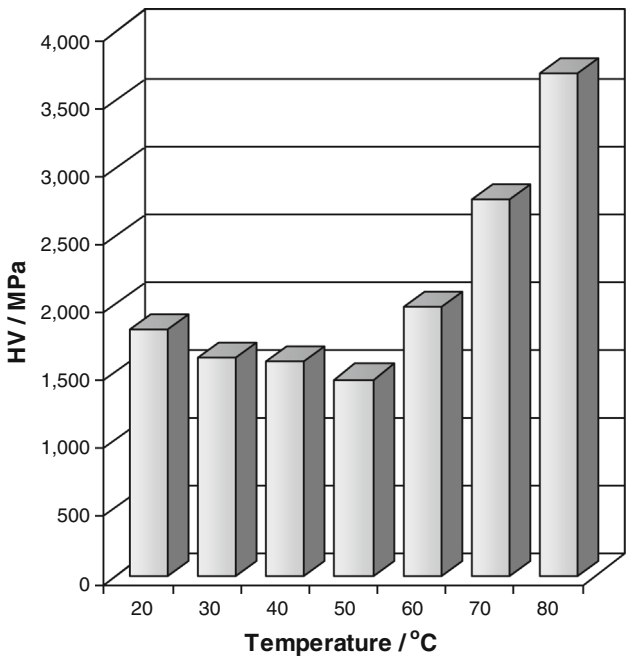

Fig. 9 Influence of temperature on microhardness (*HV*) of Mn coatings obtained from MASB with 2.20 mM of Te(VI) additive at $j_c = 15$ A dm^{-2}

levelling of the surface of the coatings was confirmed by AFM.

The increase of the temperature of manganese ammonium sulphate bath had a significant impact on the changes of current efficiency, granular composition, structure, crystallite size, and microhardness of Mn coatings. The increased temperature lead to almost double increase in current efficiency of Mn coatings and to the changes of the structure from the mixture of α-Mn and β-Mn phases to α-Mn phase. At the same time the sizes crystallite of Mn coatings decreased twice. SEM analysis revealed that the morphology of the uncertain form fine grains changes to the cube-shaped grains of Mn coatings when the temperature of manganese ammonium sulphate bath is increased.

Mn coatings obtained from manganese ammonium sulphate bath with 2.20 mM Te(VI) additive at the current density of 15 A dm^{-2} exhibited high tensile stresses. The increase of the temperature resulted in the small reduction of tensile stresses of deposits. Microhardness of Mn coatings obtained in the temperature range from 20 to 50 °C decreased insignificantly with the increase of the temperature, whereas the coatings of β-Mn phase obtained at 80 °C were very hard.

References

1. Zhang W, Cheng CY (2007) Manganese metallurgy review. Part I: leaching of ores/secondary materials and recovery of electrolytic/chemical manganese dioxide. Hydrometallurgy 89:137–159. doi:10.1016/j.hydromet.2007.08.010
2. Lu J, Dreisinger D, Glück T (2014) Manganese electrodeposition—a literature review. Hydrometallurgy 141:105–116. doi:10.1016/j.hydromet.2013.11.002
3. Gong J, Zangari G (2002) Electrodeposition and characterization of manganese coatings. J Electrochem Soc 149(4):209–217. doi:10.1149/1.1452117
4. Mulin EV, Kistosturov NI, Tarasenkova VP, Solovjov VA (1984) Influence of catholite circulation and ammonium chloride on manganese current efficiency during electrolysis. Russ J Electrochem 20(11):1429–1434
5. Agladze RI, Gofman NT (1957) Potentials of manganese electrode and its corrosion. Electrochimiya Margantsa (Russian edition) 1:5–14
6. Gonsalves M, Pletcher P (1990) A study of the electrodeposition of manganese from aqueous chloride electrolytes. J Electroanal Chem 285:185–193
7. Diaz-Arista P, Trejo G (2006) Electrodeposition and characterization of manganese coatings obtained from acidic chloride bath containing ammonium thiocyanate as an additive. Surf Coat Technol 201:3359–3367. doi:10.1016/j.surfcoat.2006.07.152
8. Diaz-Arista P, Antano-Lopez R, Measa Y, Ortega R, Chainet E, Ozil P, Trejo G (2006) EQCM study of the electrodeposition of manganese in the presence of ammonium thiocyanate in chloride-based acidic solutions. Electrochim Acta 51:4393–4404. doi:10.1016/j.electacta.2005.12.019
9. Ckonija AK, Gofman NT, Kurasvili MI, Mindin VJ (1970) Manganese electrodeposition from pure sulphate electrolyte. Electrochimiya Margantsa (Russian edition) 8:95–102
10. Gofman NT, Sadunasvili MI (1975) Manganese cathodic deposition. Electrochimiya Margantsa (Russian edition) 6:164–202
11. Gong J, Zana I, Zangari G (2001) Electrochemical synthesis of crystalline and amorphous manganese coatings. J Mater Sci Lett 20:1921–1923

12. Gong J, Zangari G (2003) Electrodeposition of sacrificial tin-manganese alloy coatings. Mater Sci Eng A 344(1–2):268–278. doi:10.1016/S0921-5093(02)00412-4
13. Wei P, Hileman OEJr, Bateni MR, Deng X, Petric A (2007) Manganese deposition without additives. Surf Coat Technol 201:7739–7745. doi:10.1016/j.surfcoat.2007.03.007
14. Agladze RI, Gofman NT (1957) Influence of some additives on manganese electrodeposition. Electrochimiya Margantsa (Russian edition) 1:53–68
15. Janickij I, Stulpinas B (1957) Electrodeposition of manganese. J Appl Chem USSR (Russian edition) 30:1776–1781
16. Lewis JR, Scaife PH, Swinkels DA (1976) Electrolytic manganese metal from chloride electrolytes. I. Effects of additives. J Appl Electrochem 6:453–462
17. Sun Y, Tian XK, He BB, Yang C, Pi ZB, Wang YX, Zhang SX (2011) Studies of the reduction mechanism of selenium dioxide and its impact on the microstructure of manganese electrodeposit. Electrochim Acta 56:8305–8310. doi:10.1016/j.electacta.2011.06.111
18. Li W, Zhang Sh (2011) In situ ellipsometric study of electrodeposition of manganese films on copper. Appl Surf Sci 257:3275–3280. doi:10.1016/j.apsusc.2010.10.155
19. Wei Q, Ren X, Du J, Wei S, Hu S (2010) Study of the electrodeposition conditions of metallic manganese in an electrolytic membrane reactor. Miner Eng 23:578–586. doi:10.1016/j.mineng.2010.01.009
20. Fan X, Xi S, Sun D, Liu Z, Jun Du, Tao C (2012) Mn–Se interactions at the cathode interface during the electrolytic-manganese process. Hydrometallurgy 127–128:24–29. doi:10.1016/j.hydromet.2012.07.006
21. Sharma RK, Rastogi AC, Singh G (2004) Electrochemical growth and characterization of manganese telluride thin films. Mater Chem Phys 84:46–51. doi:10.1016/j.matchemphys.2003.09.052
22. Sharma RK, Singh G, Shula YG, Kima H (2007) Mechanism of manganese (mono and di) telluride thin-film formation and properties. Phys B 390:314–319. doi:10.1016/j.physb.2006.08.031
23. Galvanauskaite N, Sulcius A, Griskonis E, Diaz-Arista P (2011) Influence of Te(VI) additive on manganese electrodeposition at room temperature and coating properties. Trans IMF 89:325–332. doi:10.1179/174591911X13167804920993
24. Gamburg YD, Zangari G (2011) Theory and practice of metal electrodeposition. Springer, New York
25. Ginberg AM (1984) Increasing of anticorrosion properties of metal coatings, Russian edn. Metallurgy, Moscow
26. Mattox DM (2001) Atomistic film growth and resulting film properties: residual film stress. In: Vacuum technology & coating, November 22–23
27. Kim I, Mentone PF (2006) Electroformed nickel stamper for light guide panel in LCD back light unit. Electrochim Acta 5(4):1805–1809. doi:10.1016/j.electacta.2006.01.083
28. Bozzini B, Griskonis E, Fanigliulo A, Sulcius A (2002) Electrodeposition of Zn–Mn alloys in the presence of thiocarbamide. Surf Coat Technol 154(2–3):294–303. doi:10.1016/S0257-8972(02)00010-5
29. Griskonis E, Sulcius A (2005) Influence of selenates on the electrodeposition of zinc–manganese alloy. Bull Electrochem 21(12):561–570
30. Ungiadze EM, Bogverdaze DA (1963) Lead anodes corrosion during manganese electrodepositiom. Electrochimiya Margantsa (Russian edition) 2:367–372
31. Zhang W, Bounoughaz M, Ghali E, Houlachi G (2013) Electrochemical impedance spectroscopy evaluation of behaviour of Pb–Ag anodes for zinc electrowinning. Corros Eng Sci Technol 48(6):452–460. doi:10.1179/1743278213Y.0000000091
32. Yang HT, Liu HR, Guo ZC, Chen BM, Zhang YC, Huang H, Li XL, Fu RC, Xu RD (2013) Electrochemical behavior of rolled Pb–0.8 %Ag anodes. Hydrometallurgy 140:144–150. doi:10.1016/j.hydromet.2013.10.003
33. Perkin-Elmer (1973) Analytical methods for atomic absorption spectrometry. Perkin-Elmer, Norwalk
34. Haar L, Gallagher JS, Kell GS (1984) NBS/NRC steam tables. Taylor & Francis, Levittown
35. Atkinson G, Kor SK (1965) The kinetics of ion association in manganese sulfate solutions. I. Results in water, dioxane–water mixtures, and methanol–water mixtures at 25°C. J Phys Chem 69(1):128–133. doi:10.1021/j100885a020
36. Mendez De Leo LP, Bianchi HL, Fernandez-Prini R (2005) Ion pair formation in copper sulfate aqueous solutions at high temperatures. J Chem Thermodyn 37:499–511. doi:10.1016/j.jct.2004.11.003
37. Plumridge TH, Steel G, Waigh RD (2000) Geometry-based simulation of the hydration of small molecules. Phys Chem Commun 3:36–41. doi:10.1039/B003723K
38. Samsonov AI (1982) Investigation of cathode layer during manganese electrodeposition. Dissertation, Dnepropetrovsk
39. Hurlen T, Valand T (1964) Electrochemical behavior of manganese: dissolution, deposition, hydrogen evolution. Electrochim Acta 9:1077–1085. doi:10.1016/0013-4686(64)80077-3
40. Gofman NT, Certvadze SI, Ckonija AK (1972) About dissolving manganese in aqueous solutions in the presence of ammonium ions. Electrochemistry (Russian edition) 8:1288–1294
41. Bozzini B (2000) Morphological artefacts in EDX analyses of electrodeposited Zn–Mn films. Trans IMF 78(3):93–95
42. Crozier BM, Liu Q, Ivey D (2009) Electrodeposition of an iron–cobalt phase isostructural to α-Mn. ECS Trans 16(45):141–154. doi:10.1149/1.3140017
43. Gazzara CP, Middleton RM, Weiss RJ, Hall EO (1967) Refinement of the Parameters of α manganese. Acta Crystallogr 22:859–862. doi:10.1107/S0365110X67001689
44. Finkel VA (1968) The crystal structure of manganese between 77 and 300 K. Sov Phys JETP 27(6):910–911. http://jetp.ac.ru/cgi-bin/dn/e_027_06_0910.pdf. Accessed 1 Aug 2014
45. Belinskij VN, Zosimovich DN, Kublanovskij VS (1975) Influence of impurities on manganese electrocrystallization process. Ukr Khim Zh (Russian edition) 41:1322–1325